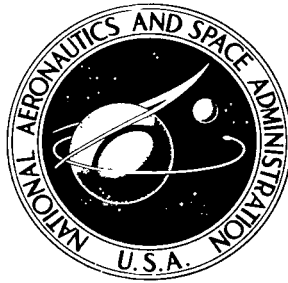


NASA TECHNICAL NOTE



NASA TN D-6448

C.1

NASA TN D-6448



LOAN COPY: RET
AFWL (DO U
KIRTLAND AFB,

THERMOELASTIC DAMPING AND ITS EFFECT ON FLUTTER OF STRESSED PANELS SITUATED IN A SUPERSONIC AIRFLOW

by R. C. Shieh

*Langley Research Center
Hampton, Va. 23365*



0132932

1. Report No. NASA TN D-6448	2. Government Accession No.	3. Recipient's Catalog No.		
4. Title and Subtitle THERMOELASTIC DAMPING AND ITS EFFECT ON FLUTTER OF STRESSED PANELS SITUATED IN A SUPERSONIC AIRFLOW		5. Report Date November 1971		
7. Author(s) R. C. Shieh	9. Performing Organization Name and Address NASA Langley Research Center Hampton, Va. 23365		6. Performing Organization Code	
12. Sponsoring Agency Name and Address National Aeronautics and Space Administration Washington, D.C. 20546	10. Work Unit No. 134-14-05-02		8. Performing Organization Report No. L-7563	
15. Supplementary Notes This research was accomplished while the author held a National Research Council Post-doctoral Resident Research Associateship at NASA Langley Research Center. Author is now at Cornell Aeronautical Laboratory, Inc., Buffalo, N.Y.	11. Contract or Grant No.		13. Type of Report and Period Covered Technical Note	
16. Abstract <p>The effects of material damping on flutter of stressed rectangular panels are studied within the context of linear thermoelasticity theory. The closed-form expression for the thermoelastic (material) damping coefficient is obtained as a function of frequency, panel temperature and dimensions, and material properties. The solution of the stability boundary-value problem is obtained by use of a generalized Galerkin method in the cross-stream direction which reduces the governing partial differential equations to a system of ordinary differential equations in the streamwise direction. These equations are then solved exactly. Numerical results are given for the thermoelastic damping coefficients and for the flutter speeds of partially and fully clamped panels subjected to midplane stress.</p>	14. Sponsoring Agency Code			
17. Key Words (Suggested by Author(s)) Thermoelastic damping Panel flutter	18. Distribution Statement Unclassified - Unlimited			
19. Security Classif. (of this report) Unclassified	20. Security Classif. (of this page) Unclassified	21. No. of Pages 32	22. Price* \$3.00	

THERMOELASTIC DAMPING AND ITS EFFECT ON FLUTTER OF STRESSED PANELS SITUATED IN A SUPERSONIC AIRFLOW

By R. C. Shieh*
Langley Research Center

SUMMARY

The effects of material damping on flutter of stressed rectangular panels are studied within the context of linear thermoelasticity theory. The closed-form expression for the thermoelastic (material) damping coefficient is obtained as a function of frequency, panel temperature and dimensions, and material properties. The solution of the stability boundary-value problem is obtained by use of a generalized Galerkin method in the cross-stream direction which reduces the governing partial differential equations to a system of ordinary differential equations in the streamwise direction. These equations are then solved exactly. Numerical results are given for the thermoelastic damping coefficients and for the flutter speeds of partially and fully clamped panels subjected to midplane stress.

INTRODUCTION

The effects of in-plane stress on panel flutter have been actively studied by many authors in recent years. Extensive references on the subject may be found in review articles (for example, refs. 1 to 5). The agreement between experimental and theoretical results has often been poor because of the difficulty in defining or measuring certain parameters (such as material and support damping, in-plane stresses, boundary-layer thickness, and support conditions) affecting the flutter boundary of a given panel. Inclusion of structural damping in theoretical flutter analyses of stressed panels is important since it may improve greatly the agreement between theoretical and experimental results. In particular, the paradoxical phenomenon of zero flutter speed predicted by theory which neglects structural damping can be removed (see refs. 6 and 7). As shown in reference 8, this paradoxical phenomenon can also be removed by accounting for the effect of initial imperfections of the panels. However, this approach is less desirable from a computational standpoint since in addition to the difficulty of defining "initial imperfections," non-linear theory is required for the analysis.

*NRC-NASA Resident Research Associate.

Structural damping for panels consists of both material damping and frictional damping at the panel supports. At present, the most widely used material-damping models in flutter analyses are either the linear viscous or hysteresis types; support damping has not been considered. Experimental evidence shows, however, that material-damping models of these types are not realistic for a wide class of metals (see ref. 9) including aluminum (see ref. 10). However, material damping can be closely predicted, based on the theory of thermoelasticity by including thermomechanical coupling, as indicated by the good correlation between experimental and theoretical results for material damping for beams (see ref. 11). Since structural damping has a significant effect on panel flutter, it seems worthwhile to study the damping mechanisms for panels and the effects of this damping in a more rigorous manner than in previous works through the use of thermoelasticity theory and through a more rational approach to the application of material and support damping. In the present paper the thermoelastic material damping mechanism, as well as the effects of such damping on panel flutter, is considered as a first step toward the aforementioned goal. Since thermoelastic damping is frequency dependent (ref. 11), inclusion of only this type of damping in panel flutter analyses cannot completely remove the contradictory phenomenon of zero flutter speed predicted by theory neglecting damping for certain special cases (ref. 6). In order to eliminate such a contradictory phenomenon completely, either frequency-independent structural damping or initial imperfections (see ref. 8) must be included in the theoretical analysis.

In the present analysis a fully or partially clamped (including simply supported) thin rectangular panel (plate) is assumed to be in a state of equilibrium under the action of uniform in-plane stresses around all edges of the panel. All surfaces of the panel are assumed to be thermally insulated for calculations of the thermoelastic damping parameters since, as shown in reference 11, the correlation between experimental and theoretical damping results based on such a thermal boundary condition is definitely better than that of an isothermal one. The lateral aerodynamic force induced by the supersonic air-flow is assumed to be given by the two-dimensional quasi-steady aerodynamic theory. The formulation of the coupled thermoelastic boundary-value problem is first presented. A closed-form expression for the thermoelastic material damping coefficient is then obtained, and the coupled governing equations are thus uncoupled. The uncoupled equations are further reduced to a system of ordinary differential equations by the use of a generalized Galerkin technique in the cross-stream direction and the resulting equations are then solved exactly. Numerical results for the thermoelastic damping coefficient and for critical flutter speeds, together with a discussion of the results, are given.

SYMBOLS

The units used for the physical quantities of this paper are given both in the International System of Units (SI) and in the U.S. Customary Units. Factors relating the two systems are given in reference 12 and those used in the present investigation are presented in appendix A. The measurements and calculations were made in U.S. Customary Units.

a panel length

$\left. \begin{matrix} a_{mn}, b_{mn} \\ c_{mn}, h_{mn} \end{matrix} \right\}$ matrices defined by equations after equation (B10)

b panel width

c_a speed of sound in undisturbed air

c_E specific heat at constant deformation of elastic solid

D plate flexural modulus, $D = \frac{Eh^3}{12(1 - \nu^2)}$

E Young's modulus

F lateral aerodynamic force (see eq. (4))

g thermomechanical coupling function, $g = g(\beta, \nu, \lambda\tau)$

g_A aerodynamic damping coefficient

g_b thermoelastic damping coefficient for a beam,

$$g_b = \beta_b \left[1 - \frac{12}{\lambda\tau_b} + \frac{24}{(\lambda\tau_b)^{3/2}} \tanh \frac{\sqrt{\lambda\tau_b}}{2} \right]$$

g_T thermoelastic damping coefficient (imaginary part of g)

h panel thickness

$h(\xi)$ function defined by equation (B4)

j, m, n	integers
K_x, K_y	rotational spring constants
k	coefficient of heat conduction
k_x, k_y	nondimensional rotational spring constants; $k_x = K_x a / D$, $k_y = K_y a / D$
M	Mach number of undisturbed airflow
M_T	thermal moment (see eq. (1))
N	number of terms of trial function in cross-stream direction (see eq. (B5))
N_T	in-plane thermal load defined by equation (8)
N_x, N_y	in-plane compressive forces per unit length of panel in x- and y-directions
\tilde{P}	in-plane loading parameter P_x / P_B at zero critical flutter speed predicted by theory which neglects damping
P_B	static buckling value of P_x
P_x, P_y	nondimensional in-plane load parameters; $P_x = N_x a^2 / D$, $P_y = N_y a^2 / D$
q	nondimensional flow speed parameter (see eqs. (24))
R	gas constant
T	temperature change from T_0
T_a	undisturbed air temperature
T_0	undisturbed equilibrium temperature (absolute) of material
T_s	absolute stagnation air temperature
t	time

\bar{t}	nondimensional time, $\bar{t} = \left(\frac{D}{\rho h a^4}\right)^{1/2} t$
U	undisturbed supersonic airflow velocity
w	lateral displacement
$X_n(\xi)$	coefficient functions in a series expansion of φ in trial functions $Y_n(\eta)$ (see eq. (B5))
x, y, z	Cartesian coordinates (see fig. 1)
$Y_n(\eta)$	trial functions in cross-stream direction; free vibration modes of an elastic beam
α	coefficient of linear thermal expansion
β, β_b	degree of thermomechanical coupling for plate and beam, respectively; $\beta = \frac{1 + \nu}{1 - \nu} \beta_b, \quad \beta_b = \frac{E \alpha^2 T_0}{\rho c_E}$
γ_a	ratio of specific heats for air
∇^2	$\nabla^2 = \frac{\partial^2}{\partial n^2} + \frac{\partial^2}{\partial y^2}$
$\bar{\nabla}^2$	$\bar{\nabla}^2 = \frac{\partial^2}{\partial \xi^2} + \frac{\partial^2}{\partial \eta^2}$
Δ_N	flutter determinant corresponding to N-terms of trial function in cross-stream direction
ϵ_{ii}	dilatational strain
$\zeta = z/h$	
$\eta = y/b$	
θ	nondimensional temperature eigenfunction

λ	nondimensional eigenvalue
λ_n	nth eigenvalue, $n = 1, 2, \dots$; $\text{Re}(\lambda_1) > \text{Re}(\lambda_2) > \text{Re}(\lambda_3) > \dots$
ν	Poisson's ratio
$\xi = x/a$	
ρ	mass density of panel
ρ_a	mass density of undisturbed air
τ	nondimensional thermal diffusion relaxation time for plate, $\tau = \omega_0 \tau^*$
τ_b	nondimensional thermal diffusion relaxation time for rectangular beam of width b , thickness h , and length l ; $\tau_b = \frac{\rho c_E h^2}{k} \left(\frac{EI}{\rho b h^4} \right)^{1/2}$
τ^*	physical thermal diffusion relaxation time for plate, $\tau^* = \left(1 + \frac{\beta}{1 - 2\nu} \right) \frac{\rho c_E h^2}{k}$
φ	nondimensional displacement eigenfunction
ω	nondimensional eigenfrequency, $\omega = \text{Im}(\lambda)$
ω_0	reference circular frequency, $\omega_0 = \left(\frac{D}{\rho h a^4} \right)^{1/2}$
ω^*	circular frequency, $\omega^* = \omega_0 \omega$
Subscript:	
cr	denotes value at flutter

ANALYSIS

Coupled Equations of Motion

Consider a fully or partially clamped rectangular panel of length a , width b , and thickness h . The panel is situated in a uniform airflow of supersonic velocity U and is subjected to the uniformly distributed in-plane compressive forces N_x and N_y

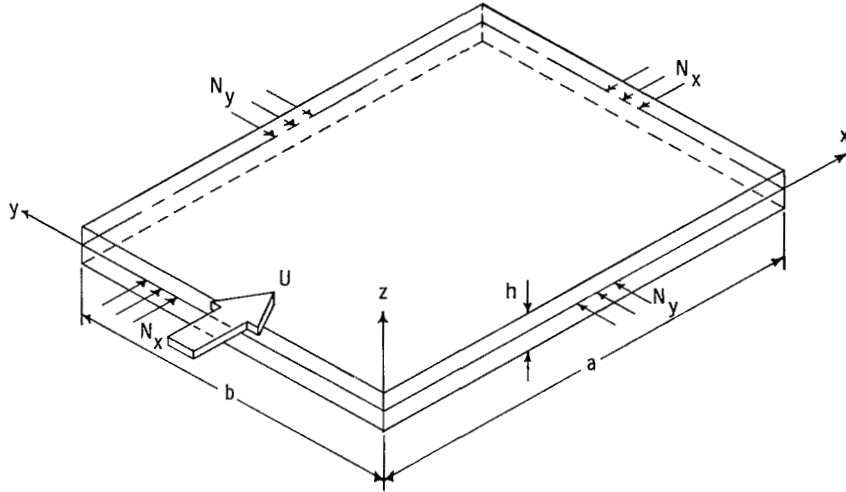


Figure 1.- Panel geometry, loads, and coordinate system.

(fig. 1). Let T be the temperature change from the constant absolute panel temperature T_0 of the undisturbed equilibrium state, and let

$$M_T = \int_{-h/2}^{h/2} E\alpha z T(x,y,z,t) dz \quad (1)$$

be the thermal moment. The temperature change T considered in this analysis is solely caused by thermomechanical coupling and, therefore, is small. Hence, the panel material constants, such as Young's modulus E and the coefficient of linear thermal expansion α in equation (1), are assumed to be independent of T (but are a function of T_0). The governing equation of small lateral vibrations of the panel is obtained by adding the inertia term $\rho h \frac{\partial^2 w}{\partial t^2}$ to equation (13.7.1) (with loading $p = N_{xy} = 0$) of reference 13 (p. 432) as follows:

$$D \nabla^2 \nabla^2 w + N_x \frac{\partial^2 w}{\partial x^2} + N_y \frac{\partial^2 w}{\partial y^2} + \frac{1}{1-\nu} \nabla^2 M_T + \rho h \frac{\partial^2 w}{\partial t^2} = F(x,y,t) \quad (2)$$

where

$$\nabla^2 = \frac{\partial^2}{\partial x^2} + \frac{\partial^2}{\partial y^2} \quad (3)$$

The aerodynamic force $F(x,y,t)$, according to the two-dimensional quasi-static aerodynamic theory, is given by (see ref. 14)

$$F(x,y,t) = -\rho_a \left(\frac{U^2}{\sqrt{M^2 - 1}} \frac{\partial w}{\partial x} + c_a \frac{\partial w}{\partial t} \right) \quad (4)$$

in which c_a is the speed of sound in air, ρ_a is the air mass density, U is the free-stream velocity, and $M = U/c_a$ is the Mach number.

If the symbols K_x and K_y are used to denote the rotational spring constants of the partially clamped edges of the panel at $x = 0, a$ and $y = 0, b$, respectively, the mechanical boundary conditions are

$$w = 0 \quad (\text{at } x = 0, a; \quad y = 0, b) \quad (5a)$$

$$D \frac{\partial^2 w}{\partial x^2} + \frac{M_T}{1 - \nu} \mp K_x \frac{\partial w}{\partial x} = 0 \quad \left(\text{at } x = \begin{Bmatrix} 0 \\ a \end{Bmatrix} \right) \quad (5b)$$

$$D \frac{\partial^2 w}{\partial y^2} + \frac{M_T}{1 - \nu} \mp K_y \frac{\partial w}{\partial y} = 0 \quad \left(\text{at } y = \begin{Bmatrix} 0 \\ b \end{Bmatrix} \right) \quad (5c)$$

For simply supported edges, $K_x = K_y = 0$ in equations (5b) and (5c). For completely clamped edges, equations (5b) and (5c) reduce to $\partial w / \partial x = \partial w / \partial y = 0$.

Heat-Conduction Equation

The temperature change T is related to the dilatational strain ϵ_{ii} and the lateral displacement w through the coupled heat-conduction equation for plates (eq. (1.12.22) of ref. 13, p. 31) given by

$$k \left(\nabla^2 T + \frac{\partial^2 T}{\partial z^2} \right) - \rho c_E \frac{\partial T}{\partial t} = \frac{E}{1 - 2\nu} \alpha T_0 \frac{\partial \epsilon_{ii}}{\partial t} \quad (6)$$

where k is the coefficient of heat conduction and c_E is the specific heat at constant deformation of the elastic solid. Within the context of the present study (i.e., the elementary plate theory of plane stress), the dilatational strain (obtained by using eqs. (8.10.4b), (8.10.7), (12.2.1), (12.2.4), and (12.2.6) of ref. 13, pp. 259, 260, 380, and 381) is

$$\epsilon_{ii} = \frac{2(1 - 2\nu)}{(1 - \nu)Eh} N_T - \frac{1 - 2\nu}{1 - \nu} z \nabla^2 w + \frac{1 + \nu}{1 - \nu} \alpha T - \frac{1 - 2\nu}{Eh} (N_x + N_y) \quad (7)$$

where

$$N_T(x, y, t) = E\alpha \int_{-h/2}^{h/2} T(x, y, z, t) dz \quad (8)$$

is the in-plane thermal load. Theoretical results for the material damping coefficients of an aluminum beam undergoing simple harmonic motion were obtained in reference 11 for an insulated thermal boundary condition (adiabatic) and an isothermal boundary condition. These results are compared with experimental measurements in figure 2. As can be seen, the experimental results correlate well with the theoretical results obtained

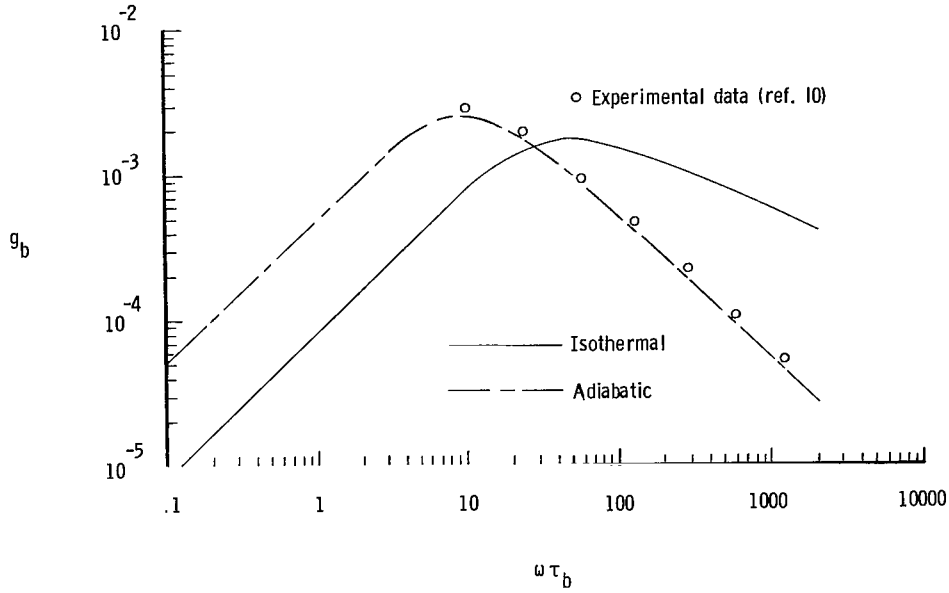


Figure 2.- Correlation of experimental measurements of material damping and theoretical calculations of thermoelastic damping coefficient for aluminum beams undergoing simple harmonic motion and subject to adiabatic and isothermal boundary conditions. (From ref. 11.)

for the insulated thermal boundary condition. Hence, the insulated thermal boundary condition will be assumed here and

$$\frac{\partial T}{\partial x} = 0 \quad (\text{at } x = 0, a) \quad (9a)$$

$$\frac{\partial T}{\partial y} = 0 \quad (\text{at } y = 0, b) \quad (9b)$$

$$\frac{\partial T}{\partial z} = 0 \quad \left(\text{at } z = \pm \frac{h}{2} \right) \quad (9c)$$

The coupled heat-conduction equation (eq. (6)) can be simplified slightly in the following manner: With the aid of equations (7), (8), and (9c), equations (6), (9a), and (9b) can be integrated over the thickness (from $z = -h/2$ to $z = h/2$) to obtain an auxiliary boundary-value problem

$$k \nabla^2 N_T - \left(\rho c_E + \frac{3E\alpha^2 T_0}{1 - 2\nu} \right) \frac{\partial N_T}{\partial t} = 0 \quad (10)$$

$$\frac{\partial N_T}{\partial x} = 0 \quad (\text{at } x = 0, a) \quad (11a)$$

$$\frac{\partial N_T}{\partial y} = 0 \quad (\text{at } y = 0, b) \quad (11b)$$

The solution of equations (10) and (11) is readily obtained as

$$N_T \equiv 0 \quad (12)$$

Physically, equation (12) indicates an antisymmetric distribution of T over the thickness. Equation (6) becomes

$$k \left(\nabla^2 T + \frac{\partial^2 T}{\partial z^2} \right) - \rho c_E \left(1 + \frac{\beta}{1 - 2\nu} \right) \frac{\partial T}{\partial t} = - \frac{\rho c_E \beta}{(1 + \nu)\alpha} z \nabla^2 \left(\frac{\partial w}{\partial t} \right) \quad (13)$$

where the nondimensional parameter

$$\beta = \frac{1 + \nu}{1 - \nu} \frac{E \alpha^2 T_0}{\rho c_E} \quad (14)$$

has been introduced. This parameter is called "the degree of thermomechanical coupling" for a reason which will become apparent later. The coupled equations of motion (eq. (2)) and heat conduction (eq. (13)), together with the boundary conditions (eqs. (5) and (9)), constitute a coupled thermoelastic stability boundary-value problem.

Coupled Eigenvalue Equations

If the nondimensional quantities

$$\left. \begin{aligned} \xi &= \frac{x}{a} \\ \eta &= \frac{y}{b} \\ \zeta &= \frac{z}{h} \\ \bar{t} &= \left(\frac{D}{\rho h a^4} \right)^{1/2} t \end{aligned} \right\} \quad (15)$$

are introduced into equations (1) to (5), (9), and (13) and the spatial and temporal variables are separated by introducing the expressions

$$\left. \begin{aligned} \frac{w}{a} &= \varphi(\xi, \eta) e^{\lambda \bar{t}} \\ \frac{T}{T_0} &= \theta(\xi, \eta, \zeta) e^{\lambda \bar{t}} \end{aligned} \right\} \quad (16)$$

into the resulting equations, the following coupled eigenvalue equations are obtained:

$$\nabla^2 \nabla^2 \varphi + P_x \frac{\partial^2 \varphi}{\partial \xi^2} + P_y \left(\frac{a}{b} \right)^2 \frac{\partial^2 \varphi}{\partial \eta^2} + 12(1 + \nu) \alpha T_0 \frac{a}{h} \int_{-1/2}^{1/2} \zeta \nabla^2 \theta \, d\zeta + q \frac{\partial \varphi}{\partial \xi} + (g_A \lambda + \lambda^2) \varphi = 0 \quad (17)$$

$$\varphi(\xi, \eta) = 0 \quad (\text{at } \xi = 0, 1; \eta = 0, 1) \quad (18)$$

$$\frac{\partial^2 \varphi}{\partial \xi^2} + 12(1 + \nu)\alpha T_0 \frac{a}{h} \int_{-1/2}^{1/2} \xi \theta \, d\xi \mp k_x \frac{\partial \varphi}{\partial \eta} = 0 \quad \left(\text{at } \xi = \begin{Bmatrix} 0 \\ 1 \end{Bmatrix} \right) \quad (19)$$

$$\left(\frac{a}{b}\right)^2 \frac{\partial^2 \varphi}{\partial \eta^2} + 12(1 + \nu)\alpha T_0 \frac{a}{h} \int_{-1/2}^{1/2} \xi \theta \, d\xi \mp k_y \frac{a}{b} \frac{\partial \varphi}{\partial \eta} = 0 \quad \left(\text{at } \eta = \begin{Bmatrix} 0 \\ 1 \end{Bmatrix} \right) \quad (20)$$

and

$$\left(\frac{h}{a}\right)^2 \nabla^2 \theta + \frac{\partial^2 \theta}{\partial \xi^2} - \lambda \tau \theta = \frac{-\beta \tau (h/a)}{(1 + \nu) \left(1 + \frac{\beta}{1 - 2\nu}\right) \alpha T_0} \xi \lambda \nabla^2 \varphi \quad (21)$$

$$\frac{\partial \theta}{\partial \xi} = 0 \quad (\text{at } \xi = 0, 1) \quad (22a)$$

$$\frac{\partial \theta}{\partial \eta} = 0 \quad (\text{at } \eta = 0, 1) \quad (22b)$$

$$\frac{\partial \theta}{\partial \xi} = 0 \quad (\text{at } \xi = 0, 1) \quad (22c)$$

where

$$\nabla^2 = \frac{\partial^2}{\partial \xi^2} + \left(\frac{a}{b}\right)^2 \frac{\partial^2}{\partial \eta^2} \quad (23)$$

The nondimensional parameters P_x , P_y , q , g_A , and τ are associated with the in-plane loads N_x and N_y , airflow speed U , aerodynamic damping coefficient $\rho_a c_a$, and the thermal diffusion relaxation time τ^* , respectively. They are defined by

$$\left. \begin{aligned} P_x &= \frac{N_x a^2}{D} \\ P_y &= \frac{N_y a^2}{D} \\ q &= \frac{\rho_a U^2}{D \sqrt{M^2 - 1}} \\ g_A &= \frac{\rho_a c_a a^4 \omega_0}{D} \\ \tau &= \omega_0 \tau^* \end{aligned} \right\} \quad (24)$$

where

$$\tau^* \equiv \left(1 + \frac{\beta}{1 - 2\nu}\right) \frac{\rho c_E h^2}{k}$$

and where

$$\omega_0 = \left(\frac{D}{\rho h a^4} \right)^{1/2} \quad (25)$$

is the reference circular frequency. The thermal diffusion relaxation time τ^* is associated with the time required for any temperature perturbation to return to the undisturbed equilibrium temperature as a result of thermal diffusion. Equations (17) to (22) govern the associated eigenvalue problem of the coupled thermoelastic-aeroelastic boundary-value problem where λ is the eigenvalue.

Reduction of Coupled Eigenvalue Equations to Uncoupled Eigenvalue Equations

For a thin panel, the thickness-length ratio h/a is much smaller than unity.

Accordingly, the in-plane heat flow term $\left(\frac{h}{a}\right)^2 \nabla^2 \theta$ in the heat-conduction equation (21) can be neglected, since its effect on the temperature eigenfunction θ is much smaller than that of the heat flow term $\partial^2 \theta / \partial \xi^2$ in the thickness direction. If the in-plane heat flow term in equation (21) is neglected, the edge thermal boundary conditions (eqs. (22a) and (22b)) cannot be prescribed arbitrarily; that is, they must be ignored. The simplified heat-conduction equation, together with the remaining thermal boundary conditions (eq. (22c)), is then solved for θ in terms of the unknown displacement eigenfunction φ , and the solution is

$$\theta(\xi, \eta, \zeta) = \frac{\beta(h/a) \nabla^2 \varphi}{\alpha T_0 (1 + \nu) \left(1 + \frac{\beta}{1 - 2\nu}\right)} \left(\zeta - \frac{\sinh \sqrt{\lambda \tau} \zeta}{\sqrt{\lambda \tau} \cosh \frac{\sqrt{\lambda \tau}}{2}} \right) \quad (26)$$

With θ known as a function of φ , equations (17), (19), and (20) can be integrated to give the following uncoupled governing equations and boundary conditions for φ :

$$(1 + g) \nabla^2 \nabla^2 \varphi + P_x \frac{\partial^2 \varphi}{\partial \xi^2} + P_y \left(\frac{a}{b}\right)^2 \frac{\partial^2 \varphi}{\partial \eta^2} + q \frac{\partial \varphi}{\partial \xi} + \lambda (g_A + \lambda) \varphi = 0 \quad (27)$$

$$\left. \begin{array}{l} \varphi = 0 \\ (1 + g) \frac{\partial^2 \varphi}{\partial \xi^2} \mp k_x \frac{\partial \varphi}{\partial \xi} = 0 \end{array} \right\} \quad (\text{at } \xi = 0, 1) \quad (28a)$$

$$\left. \begin{array}{l} \varphi = 0 \\ (1 + g) \frac{\partial^2 \varphi}{\partial \eta^2} \mp \frac{b}{a} k_y \frac{\partial \varphi}{\partial \eta} = 0 \end{array} \right\} \quad (\text{at } \eta = 0, 1) \quad (28b)$$

where

$$g = g(\beta, \nu, \lambda\tau) = \frac{\beta}{1 + \frac{\beta}{1 - 2\nu}} \left[1 - \frac{12}{\lambda\tau} + \frac{24}{(\lambda\tau)^{3/2}} \tanh \frac{\sqrt{\lambda\tau}}{2} \right] \quad (29)$$

The parameter g is the thermomechanical coupling function for thin plates since it represents the effect of thermomechanical coupling on the dynamic system. The real part of $g(\lambda\tau)$ (where λ is usually complex) represents a stiffening effect, whereas the imaginary part of $g(\lambda\tau)$ represents a damping effect. Since β appears as a factor in the expression for g , it is appropriate to refer to this parameter as the degree of thermomechanical coupling.

Equation (27) reveals that material damping (thermomechanical coupling function g) modifies only the bending term of the governing equation. Similarly, flutter equations derived on the basis of viscoelastic theory utilizing stress-strain relations for a Kelvin-Voigt body indicate that linear hysteretic structural damping should modify only those terms of the equations associated with bending (ref. 6). As pointed out in reference 6, many authors (refs. 15 to 20) have introduced a hysteretic structural damping coefficient that, in effect, is used to modify both the bending and membrane loading terms of the flutter equation. It can be shown by writing the equation of energy balance that these authors have unknowingly introduced negative membrane damping into their analyses. A comparison of the equations derived herein on the basis of thermoelasticity with those presented in reference 6 based on linear hysteretic damping reveals that the latter development neglects the stiffening effect associated with the real part of $g(\lambda\tau)$ and also completely neglects the effects of g in the rotational boundary conditions.

Solution Technique and Flutter Criterion

The uncoupled eigenvalue equations (27) and (28) cannot, in general, be solved exactly if $k_y \neq 0$. Therefore, one must resort to an approximate technique such as Galerkin's method (e.g., see ref. 21) for a solution. In the present investigation the solution method uses a generalized Galerkin's procedure (wherein only geometric boundary conditions must be satisfied) in the cross-stream (η) direction to reduce the governing partial differential equation to a system of ordinary differential equations in the streamwise (ξ) direction that approximately governs the problem. The latter equations are solved exactly. This solution method is quite general and can be applied to various panel flutter problems including, for example, the effects of arbitrary airflow direction (refs. 21 and 22). This method is more suitable than the procedure where the Galerkin method is used in both the cross-stream and streamwise directions because, with the present method, approximations are involved in one direction only. For a given accuracy, the present method usually leads to a smaller flutter determinant. The sizes of the determinants for

the present and Galerkin method are $(4N) \times (4N)$ and $(N \times J) \times (N \times J)$, respectively, where N and J are the numbers of terms in the trial functions in the cross-stream and streamwise directions, respectively. Details of the solution are given in appendix B.

NUMERICAL RESULTS AND DISCUSSION

Thermoelastic Damping

The effect of thermoelastic damping on the coupled thermoelastic-aeroelastic system is represented by the imaginary part of the thermomechanical function $g(\lambda\tau)$ (cf. eq. (29)) and is given by

$$g_T[\text{Re}(\lambda)\tau, \omega\tau, \beta, \nu] \equiv \frac{\beta}{1 + \frac{\beta}{1 - 2\nu}} \text{Im} \left[1 - \frac{12}{\lambda\tau} + \frac{24}{(\lambda\tau)^{3/2}} \tanh \frac{\sqrt{\lambda\tau}}{2} \right] \quad (\omega \equiv \text{Im}(\lambda)) \quad (30)$$

The quantity g_T is known as the "thermoelastic damping coefficient." The term in brackets is a function of $\omega\tau$ ($\omega\tau = \omega^* \tau^*$ where ω^* is the circular frequency, $\omega^* = \omega_0 \omega$). From the definitions of β (eq. (14)) and τ^* (eq. (24)), g_T at flutter is seen to be a function of the panel material properties E , ν , α , ρc_E , and k , the absolute equilibrium temperature T_0 , the panel thickness h , and the panel flutter frequency ω_{cr}^* . The effect of panel length a and width b on g_T is implicit through their effect on the flutter frequency; g_T is not an explicit function of a and b .

The variation of the ratio $\frac{g_T}{\beta / (1 + \frac{\beta}{1 - 2\nu})}$ (at flutter) with $\omega\tau$, as obtained from equation (30), is shown in figure 3. As $\omega\tau$ increases from 0 to $+\infty$, the ratio increases

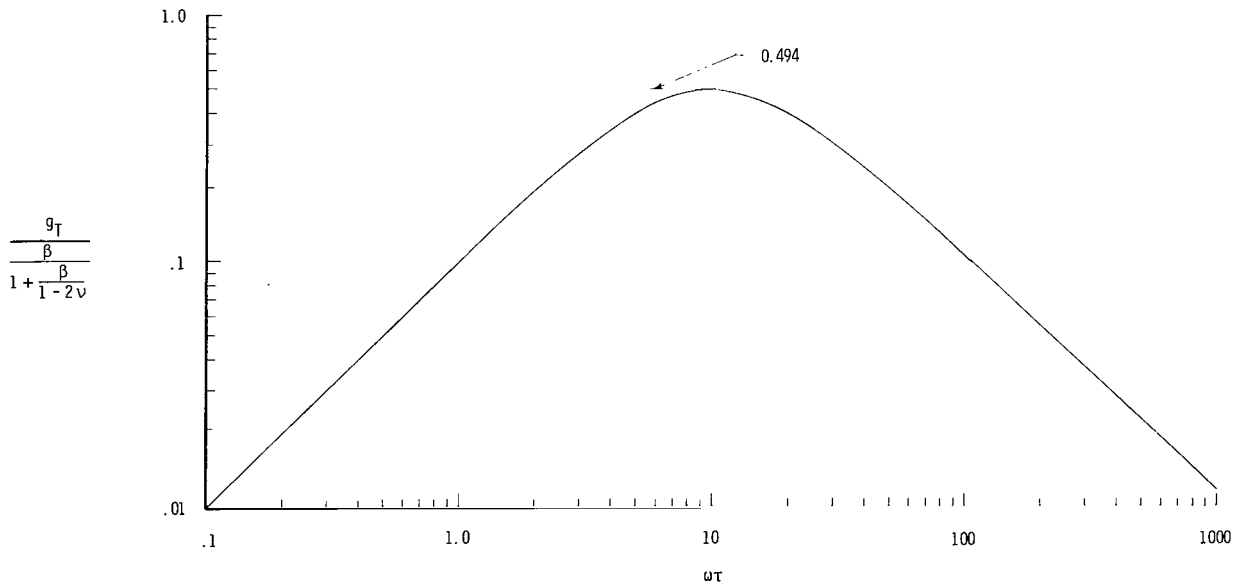


Figure 3.- Variation of thermoelastic damping coefficient with frequency for thin plates.

from 0 rapidly and monotonically to a maximum value of 0.494 at $\omega\tau = 9.9$; thereafter, it decreases monotonically to 0 at $\omega\tau = +\infty$. The material properties for 2024-T3 aluminum alloy at room temperature are as follows:

ρ	2705 kg/m ³	(5.25 slugs/ft ³)
E	72.4 GN/m ²	(10.5 × 10 ⁶ psi)
α	23 × 10 ⁻⁶ per K	(12.8 × 10 ⁻⁶ per °F)
C_E	0.84 kJ/kg-K	(0.20 Btu/lb-°F)
k	0.126 kW/m-K	(0.243 Btu-in./ft ² -s-°F)
ν		0.33

With these properties and under a room temperature $T_0 = 300$ K (540° R), the degree of thermomechanical coupling β is calculated from equation (14) to be $\beta = 0.01$, and from figure 3 the maximum value of g_T is found to be 0.0048.

The trends exhibited by the variation of the ratio $\frac{g_T}{\beta / \left(1 + \frac{\beta}{1 - 2\nu}\right)}$ with frequency

for thin plates (fig. 3) are seen to be the same as that for beams with rectangular cross sections (see fig. 2). However, it should be noted that the experiments of Bennewitz and Rötger (ref. 23) revealed that for very low frequency oscillations the value of material damping for wires may continue to decrease monotonically with decreasing frequency or begin to increase depending on the material; material damping for steel, brass, and glass decreased but results for silver and aluminum showed increases. Since that part of material damping due to plastic flow, which is neglected in the present analysis, is larger the lower the frequency, the increases in material damping at very low frequencies were attributed to plastic flow. This seems plausible since very accurate measurements have revealed the presence of permanent strains for aluminum specimens for very small stresses, whereas, for mild steel specimens, such permanent strains (if any) may be negligible (ref. 24). The experimental results of reference 23 reveal that the peak value of the material damping coefficient for aluminum wires is 2.6×10^{-3} , which occurs at $\omega\tau = 83$ Hz. These results agree extremely well with the theoretical value of the damping coefficient of 2.3×10^{-3} at $\omega\tau = 84$ Hz for thermoelastic damping (ref. 25).

The good correlation between theoretical and experimental damping results for aluminum beams (fig. 2) and for wires (refs. 23 and 25) suggests that material damping for thin aluminum panels, at least in the range of frequency for which the effects of plastic flow are negligible, consists mainly of thermoelastic damping. Hence, material damping coefficients for aluminum panels are for practical purposes given by equation (30) if $\omega\tau$ is not vanishingly small.

Measurements of structural damping for panels (e.g., ref. 26) are usually considerably greater than the thermoelastic material damping coefficients given by equation (30). However, these measurements include not only material damping but also other forms of

damping such as frictional damping at the panel supports and, in the case of built-up panels, the contribution of other forms of damping may be considerable.

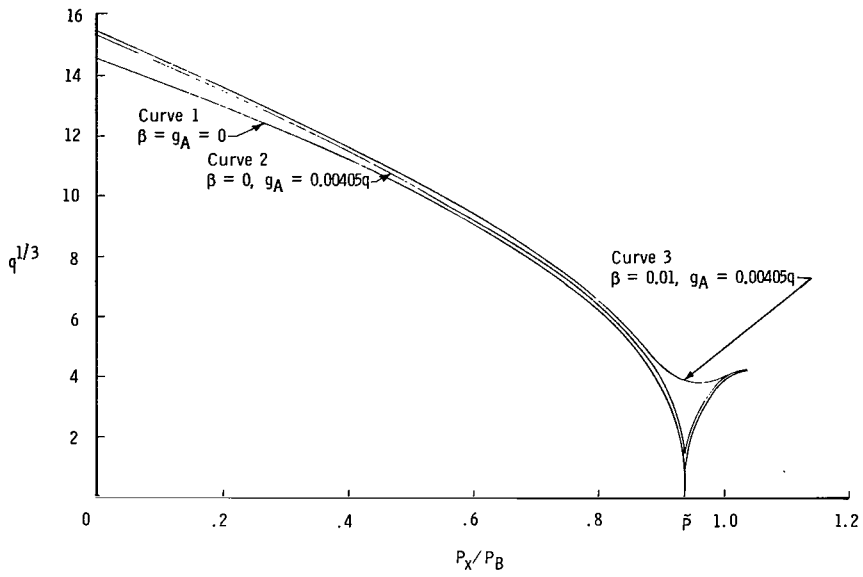
In concluding the discussion of thermoelastic material damping, it is suggested that there is a need for additional experimental effort on structural damping for beams or panels, particularly for small values of $\omega\tau$ ($\omega\tau < 10$).

Flutter Boundaries

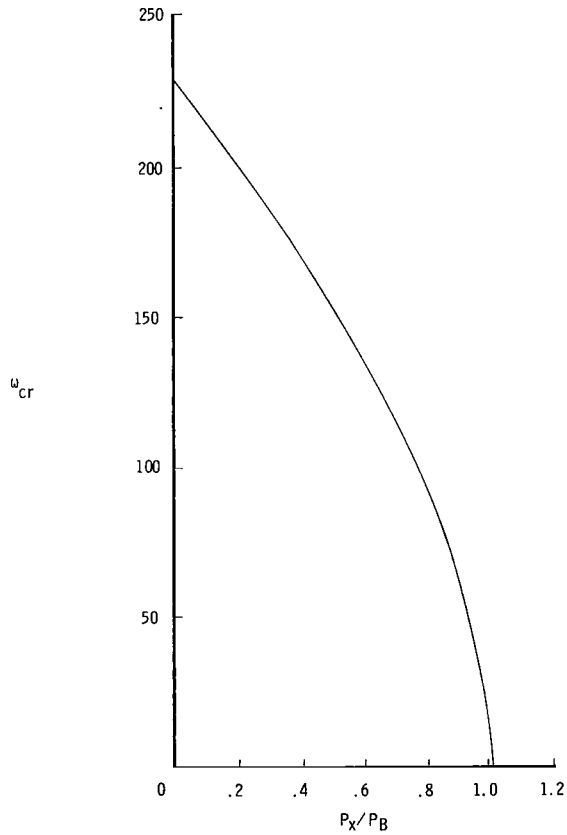
The solution procedure outlined in appendix B for finding an approximate flutter speed parameter q_{cr} has been programmed for a CDC 6600 electronic computer. The functions $Y_n(\eta)$ in the trial function $\varphi(\xi, \eta)$ given by expression (B5) are chosen to be those of free vibration modes of the elastic beam satisfying the boundary conditions (28b) with $g = 0$ (see appendix C). Numerical results for flutter speeds q_{cr} in terms of $q^{1/3}$ and flutter frequencies ω_{cr} are presented in figures 4 to 7 for flat panels of 2024-T3 aluminum alloy with thickness $h = 0.13$ cm (0.053 in.), thickness-length ratio $h/a = 0.00204$, and aspect ratios of $b/a = 0.346$ and 0.707 . The absolute undisturbed equilibrium temperature T_0 is assumed to be that of room temperature $T_0 = 300$ K (540° R) and the undisturbed airflow condition is assumed to be at a Mach number of 3 and an absolute stagnation temperature $T_s = 428$ K (770° R). These panel configurations (with $b/a = 0.346$) and flow conditions correspond to a test case given in reference 27. For these conditions and the material properties given previously for 2024-T3 aluminum alloy, the nondimensional thermal diffusion relaxation time τ is calculated to be 0.157, the aerodynamic damping coefficient g_A is calculated to be $0.00405q$ (see appendix D), and the degree of thermomechanical coupling β is calculated to be 0.01.

All flutter results are based on the two-term solution ($N = 2$ in eq. (B5)) by using the symmetric first and third free vibration modes of the elastic beam. Since the second mode is antisymmetric, inclusion of this term in the analysis has no influence on the flutter results given herein. While differences between the one- and two-term solution for the critical speed parameter $q^{1/3}$ are observed to be negligibly small for the completely clamped panel, the difference becomes somewhat significant for partially clamped panels. The maximum difference for $q^{1/3}$ corresponding to the case of curve 2 in figure 6 is 2 percent (6 percent for q itself).

Figure 4(a) shows the theoretical flutter boundaries for the completely clamped panel for undamped and damped cases. The cases for which no damping or aerodynamic damping alone is present were studied in references 14 and 28. For the undamped case (curve 1), the flutter speed q_{cr} becomes zero at $P_x/P_B = 0.94 \equiv \tilde{P}$, where P_B is the static buckling load for $q = 0$. Since the aerodynamic damping coefficient g_A is proportional to q , the presence of aerodynamic damping (cf. curve 2) has little influence on the flutter boundary for no material damping ($\beta = 0$) in the vicinity of \tilde{P} , although it does



(a) Flutter boundaries.



(b) Flutter frequency.

Figure 4.- Flutter boundaries and frequencies for a completely clamped aluminum panel.
 $b/a = 0.346$; $h/a = 0.00204$; $h = 0.13$ cm (0.053 in.); $P_y/P_x = 1$; $\tau = 0.157$.

remove the physically untenable condition of flutter at $q = 0$. The effect of thermoelastic damping (curve 3) is seen to be of considerable importance in the vicinity of \tilde{P} , although it has little influence on the flutter boundaries for smaller values of P_x/P_B and no influence at the intersection point of the flutter and buckling boundaries where $\omega = 0$ and thus $g_T = 0$.

The flutter frequencies corresponding to curve 3 of figure 4(a) are plotted in figure 4(b) as a function of the in-plane load parameter P_x/P_B . The corresponding thermoelastic damping coefficient g_T is given in figure 5 as a function of the flutter frequency ω_{cr} . As the in-plane load parameter P_x/P_B increases, flutter frequency ω_{cr} decreases (fig. 4(b)), but the damping coefficient g_T increases initially with decreasing frequency (fig. 5) and then decreases to zero at $\omega_{cr} = 0$, which corresponds to the intersection of the flutter and buckling boundaries. The value of g_T reaches its maximum value in the vicinity of $P_x/P_B = \tilde{P}$ (where $q_{cr} = 0$ when there is no damping).

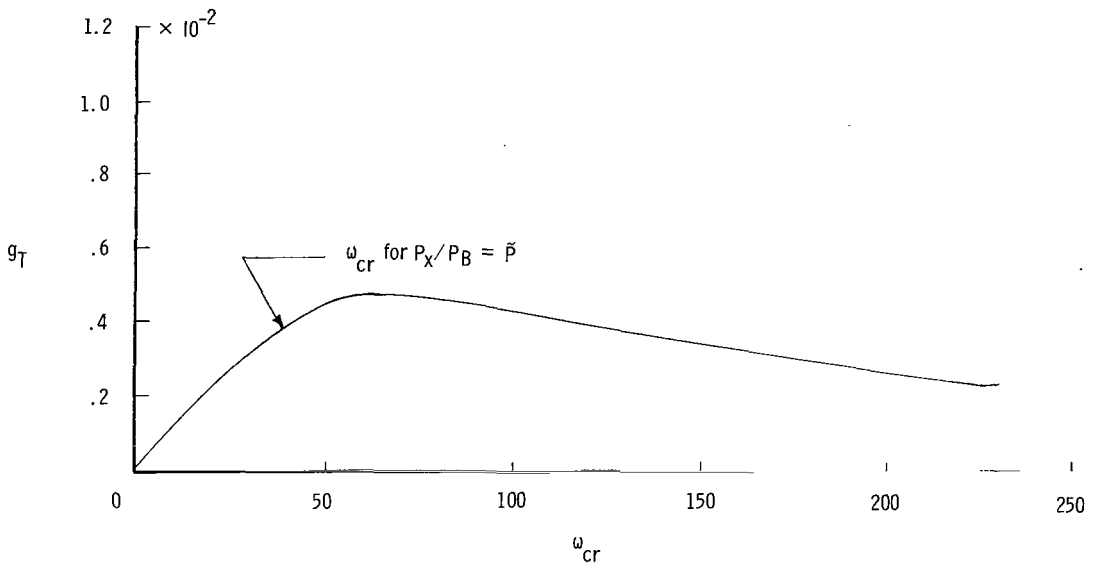


Figure 5.- Variation of thermoelastic damping coefficient with flutter frequency for the completely clamped panel considered in figure 4.

Figure 6 shows the flutter boundaries for a partially clamped aluminum panel with $k_x = k_y = 30$ for the panel configuration and panel equilibrium temperature considered in figure 4 for the completely clamped panel. Results are presented for no damping and for both aerodynamic and thermoelastic damping. (See also ref. 29 for results of undamped cases corresponding to various values of k_x and k_y .) The zero flutter speed observed for the completely clamped panel for no damping no longer appears in the present case, and the effect of damping on panel flutter is seen to become less important than for the fully clamped case. However, if the aspect ratio for the present panel is allowed to vary, it is again possible to find a case for which $q_{cr} = 0$ in the absence of all kinds of damping.

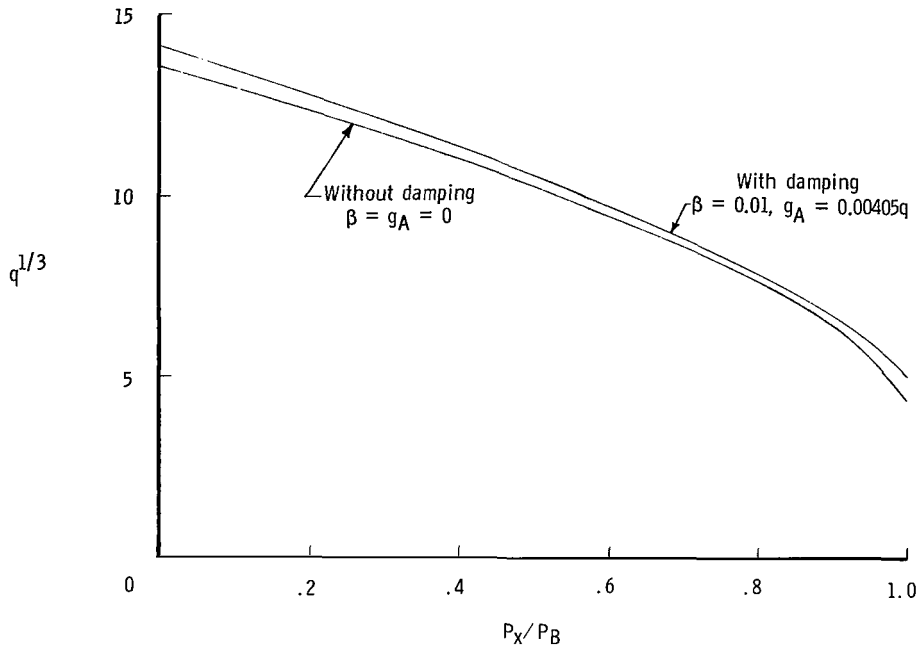


Figure 6.- Flutter boundaries for a partially clamped aluminum panel. $b/a = 0.346$; $h/a = 0.00204$; $h = 0.13$ cm (0.053 in.); $P_y/P_x = 1$; $\tau = 0.157$; $k_x = k_y = 30$.

Figure 7 shows the flutter boundaries for a simply supported panel¹ with the same airflow condition, panel equilibrium temperature, and panel configuration as considered previously except that the aspect ratio b/a is now purposely chosen to be 0.707 so that for no damping the flutter speed q_{cr} is zero at P_x/P_B . The effect of aerodynamic and thermoelastic damping is seen to be small and destabilizing.² In particular, damping has no effect at $P_x = P_B$ since the flutter frequency is zero for this condition and both aerodynamic and thermoelastic damping are frequency dependent and vanish as the frequency approaches zero. Hence, it is apparent that inclusion of only aerodynamic and thermoelastic damping in the theoretical flutter analysis cannot completely remove the paradoxical phenomenon of zero flutter speed predicted by the theory with no damping for all ranges of edge restraint and aspect ratio.

In order to remove the paradoxical phenomenon, one must include frequency-independent hysteretic material damping and support damping. An example of the existence of frequency-independent support damping is the in-plane damping caused by the in-plane kinetic dry friction force between the panel and support contacting surfaces (see refs. 32 and 33). An alternative approach is to account for possible initial imperfections

¹Equations (27) and (28) can be solved exactly for simply supported panels. (See refs. 30 and 31 for exact solution with $g_T = 0$.)

²As shown in reference 11, small amounts of thermoelastic damping may have a destabilizing effect on a nonconservative system.

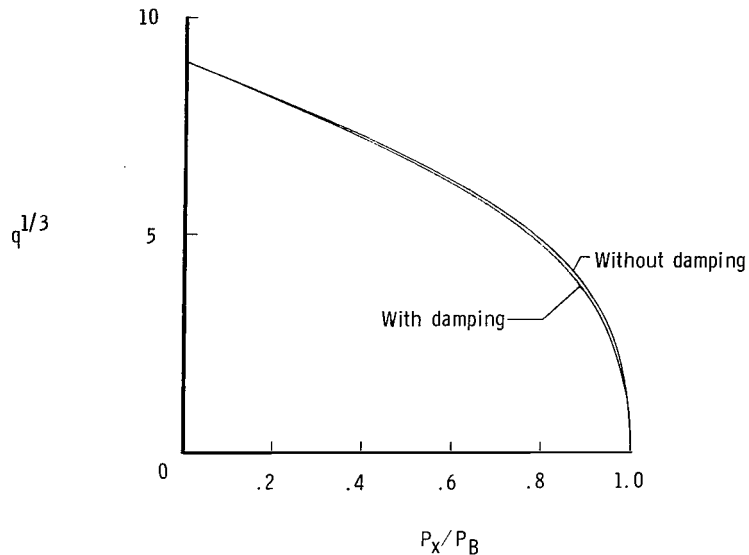


Figure 7.- Flutter boundaries for a simply supported aluminum panel.
 $b/a = 0.707$; $h/a = 0.00204$; $h = 0.13$ cm (0.053 in.); $P_y/P_x = 0$;
 $\tau = 0.157$; $\beta = 0.01$; $g_A = 0.00405q$.

in the flutter analysis (see ref. 8). This approach, as well as the case of in-plane support damping, requires a nonlinear analysis, which is beyond the scope of the present study.

CONCLUDING REMARKS

Thermoelastic material damping and its effect on the flutter of thin rectangular panels subjected to in-plane stresses in a supersonic airflow has been studied within the context of linear thermoelasticity theory. A closed-form expression for the coefficient of thermoelastic damping was obtained as a function of frequency, panel thickness, panel temperature, and material properties. The solution procedure for solving the flutter boundary-value problem consisted of application of a generalized Galerkin technique in the cross-stream direction. This reduced the governing partial differential equations to a set of uncoupled ordinary differential equations in the streamwise direction and these equations were then solved exactly.

Numerical results for the thermoelastic material damping coefficient and flutter boundaries for simply supported and partially or fully clamped panels were presented. It was shown that the importance of the effects of thermoelastic damping on flutter boundaries depends on the panel configuration and boundary conditions. Calculations were presented for a panel with a zero flutter speed (for no damping) which occurred at a frequency for which the thermoelastic damping coefficient was near its peak value. For this condition the effect of thermoelastic damping was shown to be quite significant. However, thermoelastic damping had no effect at the point where the flutter and buckling boundaries

intersect (for which the flutter frequency is zero) and may even have a destabilizing effect for certain conditions. The cases studied indicated that inclusion of thermoelastic damping, in general, may remove the anomalous behavior of zero flutter speeds predicted by flutter theory for no damping. However, this is not true when flutter speed occurs at a value of in-plane stress required for buckling. In order to remove such an anomalous behavior completely, frequency-independent structural damping must be included or effects of initial imperfections must be considered.

Langley Research Center,
National Aeronautics and Space Administration,
Hampton, Va., August 27, 1971.

APPENDIX A

CONVERSION OF U.S. CUSTOMARY UNITS TO SI UNITS

Factors required for converting the units used herein to the International System of Units (SI) are given in the following table:

Physical quantity	U.S. Customary Units	Conversion factor (*)	SI Unit (**)
Density	slugs/ft ³	515.379	kg/m ³
Force	lbf	4.448	N
Gas constant	ft ² /s ² -°F	0.1672	m ² /s ² -K
Heat energy	Btu	1054	J
Length	{ in.	0.0254	} m
	{ ft	0.3048	
Mass	{ slugs	14.59	} kg
	{ lbm	0.45359	
Specific heat	Btu/lbm-°F	4184	J/kg-K
Stress and pressure	psi = lbf/in ²	6895	N/m ²
Temperature	{ °F	(5/9)(F + 459.67)	} K
	{ °R	5/9	
Thermal conductivity	Btu-in./ft ² -s-°F	518.87	W/m-K

*Multiply value given in U.S. Customary Unit by conversion factor to obtain equivalent value in SI Unit.

**Prefixes to indicate multiples of SI units are as follows:

Prefix	Multiple
giga (G)	10 ⁹
kilo (k)	10 ³
centi (c)	10 ⁻²

APPENDIX B

SOLUTION OF THE UNCOUPLED EIGENVALUE EQUATIONS

The generalized Galerkin method (ref. 34) is employed to reduce the governing partial differential equations to a set of ordinary differential equations that approximately govern the problem. Multiplication of equations (27) and (28a) by $\delta\varphi$, the first variation of φ , and integration of the resulting equations over η from $\eta = 0$ to 1, using the integration by parts technique and the boundary conditions (28b), yield

$$\begin{aligned}
 & (1 + g) \int_0^1 \frac{\partial^4 \varphi}{\partial \xi^4} \delta\varphi \, d\eta - 2(1 + g) \left(\frac{a}{b}\right)^2 \int_0^1 \frac{\partial^2}{\partial \xi^2} \left(\frac{\partial \varphi}{\partial \eta}\right) \frac{\partial \delta\varphi}{\partial \eta} \, d\eta \\
 & + (1 + g) \left(\frac{a}{b}\right)^4 \int_0^1 \frac{\partial^2 \varphi}{\partial \eta^2} \frac{\partial^2 \delta\varphi}{\partial \eta^2} \, d\eta + \int_0^1 P_x \frac{\partial^2 \varphi}{\partial \xi^2} \delta\varphi \, d\eta \\
 & - P_y \left(\frac{a}{b}\right)^2 \int_0^1 \frac{\partial \varphi}{\partial \eta} \frac{\partial \delta\varphi}{\partial \eta} \, d\eta + q \int_0^1 \frac{\partial \varphi}{\partial \xi} \delta\varphi \, d\eta \\
 & + \lambda(\lambda + g_A) \int_0^1 \varphi \delta\varphi \, d\eta + \left(\frac{a}{b}\right)^3 h(\xi) = 0
 \end{aligned} \tag{B1}$$

$$\int_0^1 \varphi(0, \eta) \delta\varphi \, d\eta = \int_0^1 \varphi(1, \eta) \delta\varphi \, d\eta = 0 \tag{B2}$$

$$(1 + g) \int_0^1 \frac{\partial^2 \varphi}{\partial \xi^2} \mp k_x \frac{\partial \varphi}{\partial \xi} \delta\varphi \, d\eta = 0 \tag{B3}$$

where

$$h(\xi) = \left\{ \begin{array}{l} k_y \left[\frac{\partial \varphi}{\partial \eta}(\xi, 0) \frac{\partial \delta\varphi(\xi, 0)}{\partial \eta} + \frac{\partial \varphi}{\partial \eta}(\xi, 1) \frac{\partial \delta\varphi(\xi, 1)}{\partial \eta} \right] \quad (k_y \neq \infty) \\ 0 \quad (k_y = \infty, \text{ completely clamped edges}) \end{array} \right\} \tag{B4}$$

An approximate solution of equation (27) is sought in the form

$$\varphi(\xi, \eta) = \sum_{n=1}^N X_n(\xi) Y_n(\eta) \quad (N = \text{Integer} \geq 1) \tag{B5}$$

where $Y_n(\eta)$ is a set of (given) known relatively complete functions (see ref. 35) and $\varphi(\xi, \eta)$, as stipulated by the principle of virtual work, must satisfy all geometrical boundary

APPENDIX B – Continued

conditions, that is, zero displacement boundary conditions in equation (28b) if $k_y \neq \infty$ and both zero displacement and zero slope boundary conditions in equation (28b) if $k_y = \infty$ (completely clamped edge conditions). Since $Y_n(\eta)$ is a set of known (given) function, there is no variation on $Y_n(\eta)$ (that is, $\delta Y_n(\eta) = 0$ for $n = 1, 2, \dots, N$) and the variation of the function φ is

$$\delta\varphi(\xi, \eta) = \sum_{n=1}^N Y_n(\eta) \delta X_n(\xi) \quad (B6)$$

Substitution of equations (B5) and (B6) into equations (B1) to (B3), since the variation δX_n is arbitrary, leads to

$$\begin{aligned} & \sum_{n=1}^N \left\{ (1+g)a_{mn} X_n''''(\xi) - \left[2(1+g)\left(\frac{a}{b}\right)^2 b_{mn} - P_x a_{mn} \right] X_n''(\xi) + q a_{mn} X_n'(\xi) \right. \\ & \left. + \left[(1+g)\left(\frac{a}{b}\right)^4 c_{mn} - P_y b_{mn} \left(\frac{a}{b}\right)^2 + \lambda(g_A + \lambda)a_{mn} + \left(\frac{a}{b}\right)^3 h_{mn} \right] X_n(\xi) \right\} = 0 \end{aligned} \quad (B7)$$

$$\sum_{n=1}^N a_{mn} X_n(0) = \sum_{n=1}^N a_{mn} X_n(1) = 0 \quad (m = 1, 2, \dots, N) \quad (B8)$$

$$\sum_{n=1}^N a_{mn} \left[(1+g) X_n''(0) - k_x X_n'(0) \right] = 0 \quad (B9)$$

$$\sum_{n=1}^N a_{mn} \left[(1+g) X_n''(1) + k_x X_n'(1) \right] = 0 \quad (B10)$$

where

$$a_{mn} = \int_0^1 Y_m(\eta) Y_n(\eta) d\eta$$

$$b_{mn} = \int_0^1 Y_m'(\eta) Y_n'(\eta) d\eta$$

$$c_{mn} = \int_0^1 Y_m''(\eta) Y_n''(\eta) d\eta$$

$$h_{mn} = \begin{cases} k_y [Y_m'(0) Y_n'(0) + Y_m'(1) Y_n'(1)] & (k_y \neq \infty) \\ 0 & (k_y = \infty) \end{cases}$$

APPENDIX B – Continued

The general solution of the system of N -homogeneous linear differential equations (B7) is of the form

$$X_n(\xi) = \sum_{j=1}^{4N} A_{nj} e^{\Omega_j \xi} \quad (n = 1, 2, \dots, N) \quad (B11)$$

Substitution of equation (B11) into equation (B7) yields

$$\sum_{j=1}^N Q_{mj}(\Omega_n) A_{jn} = 0 \quad (m = 1, 2, \dots, N; \quad n = 1, 2, \dots, 4N) \quad (B12)$$

where

$$Q_{mn}(\Omega_j) = (1 + g) a_{mn} \Omega_j^4 - \left[\frac{2(1 + g) b_{mn} a^2}{b^2} - P_x a_{mn} \right] \Omega_j^2 + q a_{mn} \Omega_j \\ + \frac{a^4(1 + g) c_{mn}}{b^4} - \frac{a^2 P_y b_{mn}}{b^2} + \lambda(g_A + \lambda) a_{mn} + \frac{h_{mn} a^3}{b^3} \quad (B13)$$

and Ω_j are the $4N$ -roots of the determinantal equation

$$\det Q_{mn}(\Omega_j) = 0 \quad (m, n = 1, 2, \dots, N; \quad j = 1, 2, \dots, 4N) \quad (B14)$$

If A_{1n} is denoted by A_n , then equation (B14) can be solved for A_{jn} ($j = 2, 3, \dots, N$) in terms of A_n to give

$$\left. \begin{aligned} A_{jn} &= f_j(\Omega_n) A_n \\ f_1(\Omega_n) &= 1 \end{aligned} \right\} \quad (j = 1, 2, \dots, N) \quad (B15)$$

Thus, expression (B11) becomes

$$X_j(\xi) = \sum_{n=1}^{4N} f_j(\Omega_n) A_n e^{\Omega_n \xi} \quad (j = 1, 2, \dots, N) \quad (B16)$$

Finally, expression (B16), together with the $4N$ -boundary conditions (B8) to (B10), provides the following $4N$ -linear homogeneous algebraic equations in A_n :

$$\sum_{n=1}^{4N} \sum_{j=1}^N a_{mj} f_j(\Omega_n) A_n = 0 \quad (B17)$$

$$\sum_{n=1}^{4N} \sum_{j=1}^N a_{mj} f_j(\Omega_n) e^{\Omega_n \xi} A_n = 0 \quad (m = 1, 2, \dots, N) \quad (B18)$$

APPENDIX B - Continued

$$\sum_{n=1}^{4N} \sum_{j=1}^N a_{mj}(1+g)f_j(\Omega_n)\Omega_n(\Omega_n - k_x)A_n = 0 \quad (B19)$$

$$\sum_{n=1}^{4N} \sum_{j=1}^N a_{mj}(1+g)f_j(\Omega_n)\Omega_n(\Omega_n + k_x)e^{\Omega_n}A_n = 0 \quad (B20)$$

For a nontrivial solution, equations (B17) to (B20) yield the characteristic equation

$$\Delta_N[\lambda, q, g_A, P_x, P_y, g(\beta, \nu, \lambda \tau), b/a] = \det H_{mn} = 0 \quad (B21)$$

where H_{mn} is the $4N \times 4N$ coefficient matrix of A_n in equations (B17) to (B20).

Since equation (B21), in general, is a transcendental equation in λ , it yields infinitely many eigenvalues (roots) for λ ,

$$\lambda_n = \lambda_n(q, g_A, P_x, P_y, \beta, \tau, b/a) \quad (n = 1, 2, \dots) \quad (B22)$$

as functions of q , g_A , P_x , P_y , β , τ , and b/a . In the presence of damping these eigenvalues are, in general, complex. Let λ_n ($n = 1, 2, \dots$) be ordered in such a way that

$$\text{Re}(\lambda_1) \geq \text{Re}(\lambda_2) \geq \text{Re}(\lambda_3) \dots \quad (B23)$$

where $\text{Re}(\lambda_n)$ stands for "real part of λ_n ." The undisturbed equilibrium state is then said to be (see ref. 36) asymptotically stable if all the real parts of λ_n are negative (i.e., $\text{Re}(\lambda_1) < 0$), dynamically unstable (flutter) if one or more real parts of λ_n are positive and the corresponding imaginary parts of λ_n (frequencies) are nonvanishing, and statically unstable (divergence or buckling) if one or more real parts of λ_n are positive and at least one of the corresponding imaginary parts of λ_n vanishes.

For a given set of values of g_A , β , τ , b/a , ν , P_y/P_x , and P_x smaller than its static buckling value P_B , equation (B21) may be written as

$$\Delta_N(\lambda, q) = 0 \quad (B24)$$

For the numerical solution of this equation, the following method was used: The flow speed parameter q is gradually increased from 0 and the eigenvalue λ corresponding to the lowest frequency ($\text{Im}(\lambda)$) among all eigenvalues λ_n is calculated from the characteristic equation (eq. (B22)). The eigenvalue so obtained must have a negative real part in the region of stability which, for the present problems, corresponds to $q < q_{cr}$. The flutter speed q_{cr} is reached when q is increased to the value for which the real part of the eigenvalue vanishes and further increases in q result in positive real parts. If the instability is associated with the second lowest frequency, the real part of the eigenvalue associated with the lowest frequency becomes discontinuous, changes sign from negative to positive abruptly, and does not vanish for any value of q . For this case, one

APPENDIX B – Concluded

would calculate the eigenvalue associated with the second lowest frequency rather than the first and find q_{cr} so that the real part of this eigenvalue vanishes. However, for all calculations presented herein for panels, the instability was associated with the eigenvalue corresponding to the lowest frequency.

APPENDIX C

FREE VIBRATION MODES OF AN ELASTIC BEAM

The governing equations of free vibration of an elastic beam with a nondimensional length of unity and rotational spring constant k_y are obtained from equations (27) and (28) by setting $\varphi = Y(\eta)$ and $P_x = P_y = g = q = g_A = 0$ as follows:

$$\left. \begin{aligned} Y''''(\eta) + \lambda^2 Y(\eta) &= 0 \\ Y(0) = Y(1) &= 0 \\ Y''(0) - \frac{b}{a} k_y Y(0) &= 0 \\ Y''(1) + \frac{b}{a} k_y Y(1) &= 0 \end{aligned} \right\} \quad (C1)$$

The solution of equations (C1) for $k_y \neq 0$ is easily found to be

$$Y_n(\eta) = C \left[\cosh \Omega_n \eta - \cos \Omega_n \eta - \delta_n \sinh \Omega_n \eta + \left(\frac{2\Omega_n a}{k_y b} + \delta_n \right) \sin \Omega_n \eta \right] \quad (n = 1, 2, \dots) \quad (C2)$$

where C is an arbitrary constant,

$$\delta_n = \frac{\cosh \Omega_n - \cos \Omega_n + \frac{2\Omega_n \sin \Omega_n a}{k_y b}}{\sinh \Omega_n - \sin \Omega_n} \quad (C3)$$

and $\Omega_n = \text{Im}(\lambda_n)$ is the n th root of the characteristic equation

$$\begin{aligned} &\Omega_n \left[\cosh \Omega_n + \cos \Omega_n - \delta_n \sinh \Omega_n - \left(\delta_n + \frac{2\Omega_n a}{k_y b} \right) \sin \Omega_n \right] \\ &+ \frac{b}{a} k_y \left[\sinh \Omega_n + \sin \Omega_n - \delta_n \cosh \Omega_n + \left(\delta_n + \frac{2\Omega_n a}{k_y b} \right) \cos \Omega_n \right] = 0 \end{aligned} \quad (\Omega_1 < \Omega_2 < \Omega_3 < \dots) \quad (C4)$$

APPENDIX D

AERODYNAMIC DAMPING COEFFICIENT

From the definitions of q and g_A in equations (24), the aerodynamic damping coefficient is given as follows:

$$g_A = \rho_a c_a \sqrt{\frac{a^4}{\rho h D}} = \frac{\sqrt{M^2 - 1} \sqrt{D}}{c_a M^2 a} \sqrt{\frac{D}{\rho h}} q \quad (D1)$$

where the relation $M = U/c_a$ has been used. Since for air

$$c_a = \sqrt{\gamma_a R T_a} = \sqrt{\frac{\gamma_a R T_s}{1 + \frac{\gamma_a - 1}{2} M^2}} \quad (D2)$$

where the ratio of specific heats for air γ_a equals 1.4, the gas constant for air R equals $287 \text{ m}^2/\text{s}^2\text{-K}$ ($1717 \text{ ft}^2/\text{s}^2\text{-}^\circ\text{F}$), and T_s and T_a are the absolute stagnation temperature and the undisturbed air temperature, respectively, equation (D1) reduces to

$$g_A = \frac{1}{a M^2} \left[\frac{(M^2 - 1) \left(1 + \frac{\gamma_a - 1}{2} M^2\right) D}{\rho \gamma_a R h T_s} \right]^{1/2} q \quad (D3)$$

REFERENCES

1. Fung, Y. C. B.: A Summary of the Theories and Experiments on Panel Flutter. AFOSR TN 60-224, U.S. Air Force, May 1960.
2. Stocker, James E.: A Comprehensive Review of Theoretical and Experimental Panel Flutter Investigations. Rep. No. NA61H-444, North American Aviation, Inc., Sept. 15, 1961.
3. Guy, Lawrence D.; and Dixon, Sidney C.: A Critical Review of Experiment and Theory for Flutter of Aerodynamically Heated Panels. Symposium on Dynamics of Manned Lifting Planetary Entry, S. M. Scala, A. C. Harrison, and M. Rogers, eds., John Wiley & Sons, Inc., c.1963, pp. 568-595.
4. Bohon, Herman L.; and Dixon, Sidney C.: Some Recent Developments in Flutter of Flat Panels. J. Aircraft, vol. 1, no. 5, Sept.-Oct. 1964, pp. 280-288.
5. Johns, D. J.: A Survey on Panel Flutter. AGARD Adv. Rep. 1, Nov. 1965.
6. Shore, Charles P.: Effects of Structural Damping on Flutter of Stressed Panels. NASA TN D-4990, 1969.
7. Shore, Charles P.: Experimental Investigation of Flutter at Mach 3 of Rotationally Restrained Panels and Comparison With Theory. NASA TN D-5508, 1969.
8. Dowell, E. H.: Flutter of Buckled Plates at Zero Dynamic Pressure. AIAA J., vol. 8, no. 3, Mar. 1970, pp. 583-584.
9. Zener, Clarence: Elasticity and Anelasticity of Metals. Univ. of Chicago Press, c.1948.
10. Granick, Neal; and Stern, Jesse E.: Material Damping of Aluminum by a Resonant-Dwell Technique. NASA TN D-2893, 1965.
11. Shieh, R. C.: Dynamic Instability of a Cantilever Column Subjected to a Follower Force Including Thermomechanical Coupling Effect. Paper No. 71-APM-L, Amer. Soc. Mech. Eng., [1971].
12. Comm. on Metric Pract.: ASTM Metric Practice Guide. NBS Handbook 102, U.S. Dep. Com., Mar. 10, 1967.
13. Boley, Bruno A.; and Weiner, Jerome H.: Theory of Thermal Stresses. John Wiley & Sons, Inc., c.1960, pp. 31, 379-449.
14. Houbolt, John Cornelius: A Study of Several Aerothermoelastic Problems of Aircraft Structures in High-Speed Flight. Prom. Nr. 2760, Swiss Fed. Inst. Technol. (Zürich), 1958.

15. Dixon, Sidney C.: Comparison of Panel Flutter Results From Approximate Aerodynamic Theory With Results From Exact Inviscid Theory and Experiment. NASA TN D-3649, 1966.
16. Nelson, Herbert C.; and Cunningham, Herbert J.: Theoretical Investigation of Flutter of Two-Dimensional Flat Panels With One Surface Exposed to Supersonic Potential Flow. NACA Rep. 1280, 1956. (Supersedes NACA TN 3465.)
17. Dowell, E. H.; and Voss, H. M.: Theoretical and Experimental Panel Flutter Studies in the Mach Number Range 1.0 to 5.0. AIAA J., vol. 3, no. 12, Dec. 1965, pp. 2292-2304.
18. Johns, D. J.; and Parks, P. C.: Effect of Structural Damping on Panel Flutter. Aircraft Eng., vol. XXXII, no. 380, Oct. 1960, pp. 304-308.
19. Kobett, D. R.; and Zeydel, E. F. E.: Research on Panel Flutter. NASA TN D-2227, 1963.
20. Cunningham, Herbert J.: Flutter Analysis of Flat Rectangular Panels Based on Three-Dimensional Supersonic Unsteady Potential Flow. NASA TR R-256, 1967.
21. Kordes, Eldon E.; and Noll, Richard B.: Theoretical Flutter Analysis of Flat Rectangular Panels in Uniform Coplanar Flow With Arbitrary Direction. NASA TN D-1156, 1962.
22. Bohon, Herman L.: Flutter of Flat Rectangular Orthotropic Panels With Biaxial Loading and Arbitrary Flow Direction. NASA TN D-1949, 1963.
23. Bennewitz, K.; and Rötger, H.: Über die innere Reibung fester Körper; Absorptionsfrequenzen von Metallen im akustischen Gebiet. Phys. Z., Jahrg. 37, Nr. 16, Aug. 15, 1936, pp. 578-588.
24. Prager, William; and Hodge, Philip G., Jr.: Theory of Perfectly Plastic Solids. Dover Publ. Inc., c.1968, pp. 2 and 6.
25. Zener, C.; Otis, W.; and Nuckolls, R.: Internal Friction in Solids. III. Experimental Demonstration of Thermoelastic Internal Friction. Phys. Rev., Second ser., vol. 53, Jan. 1, 1938, pp. 100-101.
26. Hess, Robert W.: Experimental and Analytical Investigation of the Flutter of Flat Built-Up Panels Under Streamwise Inplane Load. NASA TR R-330, 1970.
27. Shideler, John L.; Dixon, Sidney C.; and Shore, Charles P.: Flutter at Mach 3 of Thermally Stressed Panels and Comparison With Theory for Panels With Edge Rotational Restraint. NASA TN D-3498, 1966.

28. Voss, H. M.; and Dowell, E. H.: Effect of Aerodynamic Damping on Flutter of Thin Panels. AIAA J., vol. 2, no. 1, Jan. 1964, pp. 119-120.
29. Erickson, Larry L.: Supersonic Flutter of Flat Rectangular Orthotropic Panels Elastically Restrained Against Edge Rotation. NASA TN D-3500, 1966.
30. Hedgepeth, John M.: Flutter of Rectangular Simply Supported Panels at High Supersonic Speeds. J. Aeronaut. Sci., vol. 24, no. 8, Aug. 1957, pp. 563-573, 586.
31. Movchan, A. A.: On the Stability of a Panel Moving in a Gas. NASA RE 11-21-58W, 1959.
32. Mentel, T. J.: Vibrational Energy Dissipation at Structural Support Junctions. Structural Damping, Jerome E. Rozicka, ed., Am. Soc. Mech. Engrs., c.1959, pp. 89-116.
33. Ungar, Eric E.: Energy Dissipation at Structural Joints; Mechanisms and Magnitudes. FDL-TDR-64-98, U.S. Air Force, Aug. 1964.
34. Fung, Y. C.: Foundations of Solid Mechanics. Prentice-Hall, Inc., 1965, pp. 338-339.
35. Sokolnikoff, I. S.: Mathematical Theory of Elasticity. Second Ed., McGraw-Hill Book Co., Inc., 1956, pp. 404-411.
36. Minorsky, Nicholas: Nonlinear Oscillations. D. Van Nostrand Co., Inc., c.1962, pp. 144-145.



012 001 C1 U 32 711105 S00903DS
DEPT OF THE AIR FORCE
AF WEAPONS LAB (AFSC)
TECH LIBRARY/WLOL/
ATTN: E LOU BOWMAN, CHIEF
KIRTLAND AFB NM 87117

POSTMASTER: If Undeliverable (Section 158
Postal Manual) Do Not Return

"The aeronautical and space activities of the United States shall be conducted so as to contribute . . . to the expansion of human knowledge of phenomena in the atmosphere and space. The Administration shall provide for the widest practicable and appropriate dissemination of information concerning its activities and the results thereof."

— NATIONAL AERONAUTICS AND SPACE ACT OF 1958

NASA SCIENTIFIC AND TECHNICAL PUBLICATIONS

TECHNICAL REPORTS: Scientific and technical information considered important, complete, and a lasting contribution to existing knowledge.

TECHNICAL NOTES: Information less broad in scope but nevertheless of importance as a contribution to existing knowledge.

TECHNICAL MEMORANDUMS: Information receiving limited distribution because of preliminary data, security classification, or other reasons.

CONTRACTOR REPORTS: Scientific and technical information generated under a NASA contract or grant and considered an important contribution to existing knowledge.

TECHNICAL TRANSLATIONS: Information published in a foreign language considered to merit NASA distribution in English.

SPECIAL PUBLICATIONS: Information derived from or of value to NASA activities. Publications include conference proceedings, monographs, data compilations, handbooks, sourcebooks, and special bibliographies.

TECHNOLOGY UTILIZATION PUBLICATIONS: Information on technology used by NASA that may be of particular interest in commercial and other non-aerospace applications. Publications include Tech Briefs, Technology Utilization Reports and Technology Surveys.

Details on the availability of these publications may be obtained from:

SCIENTIFIC AND TECHNICAL INFORMATION OFFICE

NATIONAL AERONAUTICS AND SPACE ADMINISTRATION

Washington, D.C. 20546